τ PRODUCTION AND DECAY WITH THE CELLO DETECTOR AT PETRA

Cello Collaboration

H.J. BEHREND, L. CRIEGEE, J.B. DAINTON [1], J.H. FIELD [2], G. FRANKE, H. JUNG [3], J. MEYER, V. SCHRÖDER, G.G. WINTER
Deutsches Elektronen-Synchrotron, DESY, D-2000 Hamburg 52, Fed. Rep. Germany

P.J. BUSSEY, C. BUTTAR [4], A.J. CAMPBELL, D. HENDRY, J.M. SCARR, I.O. SKILLICORN, K.M. SMITH
University of Glasgow, Glasgow G12 8QQ, UK

J. AHME, V. BLOBEL, W. BREHM, M. FEINDT, H. FENNER, J. HARJES, J.H. PETERS, O. PODOBRIN, H. SPITZER
II. Institut für Experimentalphysik, Universität Hamburg, D-2000 Hamburg, Fed. Rep. Germany

W.D. APEL, J. ENGLER, G. FLÜGGE [3], D.C. FRIES, J. FUSTER [5], P. GABRIEL, K. GAMERDINGER [6], P. GROSSE-WIESMANN [7], M. HAHN, U. HÄDINGER, J. HANSMEYER, H. KÜSTER [8], H. MÜLLER, K.H. RANITZSCH, H. SCHNEIDER, R. SEUFERT
Kernforschungszentrum Karlsruhe and Universität Karlsruhe, D-7500 Karlsruhe, Fed. Rep. Germany

W. DE BOER, G. BUSCHHORN, G. GRINDHAMMER [7], B. GUNDERSON, C. KIESLING [9], R. KOTTHAUS, H. KROHA, D. LÜERS, H. OBERLACK, P. SCHACHT, S. SCHOLZ, G. SHOOSHTARI, W. WIEDENMANN
Max-Planck-Institut für Physik und Astrophysik, D-8000 Munich 40, Fed. Rep. Germany

M. DAVIER, J.F. GRIVAZ, J. HAISSINSKI, P. JANOT, V. JOURNÉ, D.W. KIM, F. LE DIBERDER, J.J. VEILLET
Laboratoire de l'Accélérateur Linéaire, F-91405 Orsay, France

K. BLOHM, R. GEORGE, M. GOLDBERG, O. HAMON, F. KAPUSTA, L. POGGIOLI, M. RIVOAL
Laboratoire de Physique Nucléaire et Hautes Energies, Université de Paris, F-72230 Paris Cedex 05, France

G. D'AGOSTINI, F. FERRAROTTO, M. IACOVACCI, B. STELLA
University of Rome and INFN, I-00185 Rome, Italy

G. COZZIKA, Y. DUCROS
Centre d'Études Nucléaires, Saclay, F-91191 Gif-sur-Yvette Cedex, France

G. ALEXANDER, A. BECK, G. BELLA, J. GRUNHAUS, A. KLATCHKO, A. LEVY and C. MILSTÉNE
Tel Aviv University, 69978 Tel Aviv, Israel

Received 22 February 1989

The reaction $e^+e^- \to \tau^+\tau^-$ has been studied at centre of mass energies between 14.0 and 46.8 GeV with the CELLO detector at the PETRA e^+e^- collider. We present results for the cross section σ_τ and the charge asymmetry A_τ. The results are in good agreement with the standard model. We have also measured the topological decay rates BR_1, BR_3 and BR_5 for the inclusive decay of the τ lepton into one, three and five charged particles. The results confirm and improve earlier CELLO measurements at other energies. We find for the combined values at all energies $BR_1 = (84.9 \pm 0.4 \pm 0.3)\%$, $BR_3 = (15.0 \pm 0.4 \pm 0.3)\%$ and $BR_5 = (0.16 \pm 0.13 \pm 0.04)\%$.

1. Introduction

τ pair production in e^+e^--annihilations is a useful process for testing various aspects of the standard model [1]. The measurement of the charge asymmetry in the differential cross section for τ pair production allows a determination of the axial vector coupling constant a_τ, whereas cross section and polarization measurements give information on the vector coupling constant v_τ. The results therefore provide a sensitive test of lepton universality and of the neutral current structure.

The decay of the τ lepton proceeds via the charged current interaction. The branching ratios for the major decay channels are also predicted by the standard model. Measurements of the exclusive decay widths and of the decay widths into 1, 3, 5, etc. charged particles plus neutrals, the so-called topological branching ratios, provide further tests of the nature of the τ and allow for a powerful consistency check of the experimental data. Recently, a discrepancy has been reported between the sum of the branching ratios for the exclusive decays of the τ into one charged particle plus neutrals and the corresponding topological branching ratio for one-prong decays [2].

We have performed measurements of the τ pair production cross section and topological branching ratios of the τ at centre of mass (CM) energies between 14.0 GeV and the highest PETRA energy of 46.8 GeV. Results from data taken at CM energies of 14,22 and 34.2 GeV have already been reported [3–5]. New data were collected between CM energies of 35–46.8 GeV. In what follows we refer to the new data sample unless otherwise mentioned.

2. Experiment

CELLO is a general purpose magnetic detector, equipped with a fine-grain lead–liquid-argon electromagnetic calorimeter. Charged particles are measured over 91% of the full solid angle in a cylindrical detector made of interleaved drift and proportional chambers in a 1.3 T magnetic field, yielding a momentum resolution of $\sigma(p)/p = 0.02\,p$ (p in GeV/c) without vertex constraint and $0.01\,p$ with vertex constraint. For neutral-particle detection and charged-lepton identification we use the barrel part of the calorimeter which covers a solid angle of 86% of 4π. Each of the sixteen calorimeter modules samples in depth the energy deposited by particles in the liquid argon. Up to a maximum of 20 radiation lengths for normal incidence, the charge is collected on lead strips of three different orientations. For each shower this information is combined to give seven samplings in depth. The energy resolution is $\sigma(E)/E = 0.05 + 0.10/\sqrt{E}$ (E in GeV), and the angular resolution varies from 6 to 10 mrad. Muons are detected behind an 80 cm thick iron absorber by large planar drift chambers covering 92% of 4π. The spatial resolution of these chambers is 0.6 cm. A detailed description of the detector can be found elsewhere [6].

The new data sample corresponds to a total integrated luminosity of 135.7 pb^{-1} where the bulk of the data (87.0 pb^{-1}) was taken at a fixed energy of 35.0

[1] Permanent address: University of Liverpool, Liverpool L 69 3BX, UK.
[2] Present address: Université de Genève, CH-1211 Geneva 4, Switzerland.
[3] Present address: RWTH, D-5100 Aachen, Fed. Rep. Germany.
[4] Present address: Oxford University, Oxford OX1 3RM, UK.
[5] Present address: Instituto de Física Corpuscular, Universidad de Valencia, Valencia, Spain.
[6] Present address: MPI München, D-8000 Munich 40, Fed. Rep. Germany.
[7] Present address: SLAC, Stanford, CA 94305, USA.
[8] DESY, D-2000 Hamburg 52, Fed. Rep. Germany.
[9] Heisenberg-Stipendiat der Deutschen Forschungsgemeinschaft.

GeV. The rest of the data (48.7 pb^{-1}) was taken in an energy scan ranging from 35.0 to 46.8 GeV and corresponding to an average CM energy of 42.8 GeV. Because of different experimental conditions our new data sample is subdivided into six energy bins for the measurement of the total loss section, and three energy bins for the charge asymmetry measurement. Each bin corresponds to specific PETRA running periods at different CM energies between the autumn of 1982 and the end of 1986.

The CELLO detector is able to detect all τ decay channels. In our selection, however, we did not attempt to include τ pairs where both τ leptons decay into either electrons or muons. These channels, representing only 6% of all final states, are heavily contaminated by Bhabha scattering, two-photon annihilation into lepton pairs or μ pair production.

τ events are characterised by energy and momentum imbalance in the event and low multiplicity final states with energetic particles. For the selection procedure the event topology is defined using the sphericity axis calculated from all observed charged and neutral particles. The particles are grouped into two jets divided by the plane perpendicular to the sphericity axis. For each jet ($i=1,2$) the total momentum vector $\boldsymbol{q}_i=\sum_j \boldsymbol{p}_{ij}$, the total charge Q_i and the total invariant mass m_i (including photons and assuming pions for the charged particles) are calculated. The true charged multiplicity in each jet is restored by identifying electron–positron pairs from γ conversions in the beampipe or in the chambers. A cut of 80 MeV for the invariant mass of the e^+e^- pair was employed to define a converted photon.

Electrons were identified via their characteristic shower pattern in the calorimeter and by comparing the total energy with the momentum measured in the track detector. For the identification of muons a hit in the muon chambers and a shower profile in the calorimeter compatible with the expectation for a minimum ionizing particles were demanded. The efficiency to identify an electron (muon) was 68% (72%) averaged over all momenta [7].

For the event selection we proceed as follows: A cut in the acollinearity angle α_{acol} between the jet momentum vectors $\boldsymbol{q}_i$ ($0.5^\circ<\alpha_{\mathrm{acol}}<50^\circ$) removes a large part of Bhabha, μ pair, cosmic ray, two photon and radiative τ pair events. The remaining background from two photon collisions is removed by a cut in acoplanarity ($0^\circ<\alpha_{\mathrm{acop}}<40^\circ$), and by requesting a minimum energy ($E>0.05\cdot\sqrt{s}$) in the central barrel calorimeter. This cut also removes beam–gas events. Multihadronic events are almost completely eliminated by restricting the maximum number of charged particles to 10 and limiting the invariant mass per jet to less than 2.7 GeV/c^2. Finally, cosmic ray events are efficiently removed by demanding for a minimum opening angle of 0.5° in the Rz-projection between the tracks in the wire chamber. Additional cuts taking into account the longitudinal shower development in the calorimeter have been used in order to remove efficiently events with only electrons in the final state. For further details of the selection algorithm see ref. [7].

These selections yielded 6144 candidates which were all subjected to a visual scan. In the scan 2028 remaining background events were removed. These events were Bhabhas or events with two low energy electrons in the final state originating from either two-photon collisions or τ pair production (50%), events with unreconstructed particles outside the acceptance required in the selection procedure, or with badly reconstructed particle tracks inside the acceptance (14%), and cosmic ray events (10%). Further contributions came from radiative two-muon events (18%), multihadronic events (6%) and beam–gas events (2%). A final sample of 4116 events was obtained.

The residual background contamination of the accepted event sample was estimated using full Monte Carlo simulations for the background channels including scanning. The various selection efficiencies and event contribution to the data sample are listed in table 1. The total background is estimated to be 6.7%.

The efficiencies of the selection procedure were determined by Monto Carlo methods using a detailed simulation of the reaction $e^+e^-\to\tau^+\tau^-(\gamma)$ in the CELLO detector. We have used a four-vector generator incorporating spin effects of the final state τ's [8]. All known τ decay channels have been simulated with the measured branching ratios [3,4,9]. The events were then passed through the same reconstruction and analysis programs as the real data. An overall selection efficiency, including the scanning, of 46% is obtain within our acceptance. The scanning efficiency was determining to be 93% for two-prong

Table 1
Efficiencies and contributions to the data sample for signal and background processes.

Process	$\langle\epsilon\pm\Delta\epsilon\rangle$ [a]	Contribution	
		%	events
$e^+e^-\to\tau^+\tau^-(n\gamma)$ $n=0,1$	0.341 ± 0.004	93.3 ± 1.1	3841.6 ± 45.3
$e^+e^-\to e^+e^-(n\gamma)$ $n\geq0$	$(2.5\ \pm0.7)\times10^{-4}$	2.5 ± 0.7	103.5 ± 29.0
$e^+e^-\to\mu^+\mu^-(n\gamma)$ $n=0,1$	$(2.1\ \pm0.3)\times10^{-3}$	0.6 ± 0.1	$26.3\pm\ 4.4$
$e^+e^-\to q\bar{q}(n\gamma)$ $n=0,1$	$(5.4\ \pm1.3)\times10^{-4}$	0.5 ± 0.1	$18.7\pm\ 3.7$
$e^+e^-\to e^+e^-e^+e^-$	$(0.0\ \pm4.0)\times10^{-5}$	0.0 ± 0.0	$0.0\pm\ 0.0$
$e^+e^-\to e^+e^-\mu^+\mu^-$	$(1.3\ \pm0.9)\times10^{-4}$	1.1 ± 0.8	46.5 ± 33.8
$e^+e^-\to e^+e^-\tau^+\tau^-$	$(4.6\ \pm0.6)\times10^{-3}$	1.7 ± 0.2	$69.8\pm\ 8.2$
$e^+e^-\to e^+e^-q\bar{q}$	$(7.2\ \pm5.7)\times10^{-5}$	0.3 ± 0.2	$9.7\pm\ 6.5$

[a] Including acceptance.

events and 96% for multi-prong events. The trigger efficiency was derived by comparing redundant trigger modes and was cross-checked by Monte Carlo calculations. It amounts to 98.5% for the two-prong and better than 99% for the multi-prong events.

3. Results

3.1. Topological branching ratios

From the previous discussion it is evident that a τ decaying into m charged particles can be detected in various charged topologies. For example, our algorithm for the identification of converted photons may fail to find the conversion pair owing to measurement errors or may misidentify a pion pair as an e^+e^- pair. Furthermore tracks may overlap or may escape detection due to limited acceptance. Thus, in general the true number N_{mj} of τ pairs where one τ decays into m and the other one into j charged particles is related to the number τ pairs n_{lk} expected to be seen in the detector by

$$n_{lk}=\sum_{mj}\epsilon_{kl\leftarrow mj}N_{mj}\quad(l,k=1,2,3,\ldots)\,,$$

$$N_{mj}=N_{\rm tot}\cdot 2{\rm BR}_m{\rm BR}_j\quad(m\neq j,\ m,j=1,3,5)\,,$$

$$N_{mm}=N_{\rm tot}\cdot{\rm BR}_m^2\,. \qquad (1)$$

$N_{\rm tot}$ is the total number of τ pairs, corrected for all efficiencies and the full solid angle, and the BR_m are the topological branching ratios for the decay into m charged particles. $\epsilon_{lk\leftarrow mj}$ represents the probability to detect τ pairs with charge topology mj as τ pairs with topology lk. This matrix $\{\epsilon_{lk\leftarrow mj}\}$ was determined by Monte Carlo methods and receives contributions from reconstruction, selection, scanning and trigger inefficiencies. The matrix is shown in table 2.

In the new sample we observe 64.8% of events in the 1-1 topology, 13.0% as 1-2, 18.2% as 1-3, 0.8% as 1-4, 0.2% as 1-5, 1.8% as 2-3 and 1.2% as 3-3. The number m_{lk} of events actually observed in the detector is Poisson-distributed around the expectation n_{lk}. We therefore determine the parameters $N_{\rm tot}$, BR_1, BR_3, BR_5 by minimising the likelihood function

$$\mathcal{F}=-\ln\prod_{(l,k)}\mathcal{P}(m_{lk})$$

$$=-\sum_{lk}\ln\left(\frac{(n_{lk})^{m_{lk}}}{m_{lk}!}\exp(-n_{lk})\right). \qquad (2)$$

The topological branching fractions into one, three, and five charged particles from the data taken at a fixed energy of 35.0 GeV and at an average CM energy of 42.8 GeV [7] are in good agreement with our earlier measurements at CM energies of 14, 22 [4] and 34 GeV [3] (see table 3). We therefore combine the above measurements and obtain

$${\rm BR}_1=(84.9\pm0.4\pm0.3)\ [\%]$$

$${\rm BR}_3=(15.0\pm0.4\pm0.3)\ [\%]$$

$${\rm BR}_5=(0.16\pm0.13\pm0.04)\ [\%]\,. \qquad (3)$$

Our results agree with recent measurements from TASSO [10] and TPC [11]. The branching ratio BR_1, however, is smaller than results from other re-

Table 2

	1-1	1-3	1-5	3-3	3-5	5-5
1-1	30.17±0.25	1.84±0.10	1.19±0.53	0.05±0.05	0.00±1.04	0.46±0.46
1-2	1.45±0.05	10.81±0.24	3.81±0.96	1.11±0.25	0.00±1.04	0.00±0.46
1-3	0.37±0.03	27.50±0.38	4.95±1.08	2.68±0.38	0.00±1.04	0.00±0.46
1-4	0.03±0.01	0.75±0.06	19.29±2.15	0.06±0.06	1.04±1.04	1.83±0.91
1-5	0.01±0.004	0.12±0.03	7.74±1.35	0.05±0.05	0.00±1.04	0.46±0.46
1-6	0.00±0.002	0.00±0.01	0.97±0.48	0.00±0.05	0.00±1.04	0.00±0.46
2-3	0.01±0.004	0.53±0.05	0.00±0.25	15.15±0.91	2.07±1.47	3.20±1.21
2-5	0.00±0.002	0.00±0.01	0.00±0.25	0.00±0.05	4.13±2.06	1.83±0.91
3-3	0.00±0.002	0.13±0.03	0.00±0.25	18.48±1.01	5.16±2.31	2.74±1.12
3-4	0.00±0.002	0.00±0.01	0.00±0.25	1.55±0.29	14.42±3.85	8.68±1.99
3-5	0.00±0.002	0.00±0.01	0.25±0.25	0.16±0.09	6.19±2.53	1.37±0.79
3-6	0.00±0.002	0.00±0.01	0.00±0.25	0.00±0.05	1.04±1.04	0.00±0.46
4-5	0.00±0.002	0.00±0.01	0.00±0.25	0.00±0.05	0.00±1.04	5.02±1.51
5-5	0.00±0.002	0.00±0.01	0.00±0.25	0.00±0.05	0.00±1.04	0.46±0.46

Table 3
Measurements of the topological branching ratios (in %) of the τ lepton. The errors quoted are statistical and systematic ones.

BR_1	BR_3	BR_5	$\sqrt{s}$	Ref.
84.0±2.0 [a]	15.0±2.0 [a]	1.0 ±0.4 [a]	34	[3]
85.2±2.6±1.3	14.8±2.0±1.3	<1.0(95% CL)	14	[4]
85.1±2.8±1.3	14.5±2.2±1.3	<1.0(95% CL)	22	[4]
84.5±0.9±0.8	15.4±0.9±0.8	<0.5(95% CL)	42.8	[7]
85.0±0.5±0.3	14.9±0.5±0.3	0.16±0.13±0.04	35.0	b)
84.9±0.4±0.3	15.0±0.4±0.3	0.16±0.13±0.04	all	b)

[a] Statistical and systematic error added in quadrature. [b] This analysis.

cent experiments at PETRA [12,13] and PEP [14–16]. Correspondingly, BR_3 is larger by 2% compared to those experiments. The significance of the discrepancy between our data and the previous world average is 3.4 standard deviations (see fig. 1). Our five-prong branching ratio is in accordance with the very small experimental value for the five-prong branching ratio from other experiments [19] and we observe no candidate with a higher topology than five, consistent with the existing experimental limits [20,9].

It should be noted that the determination of the branching ratios with the method described above is not affected by luminosity errors. This is important in reducing the systematic uncertainties. We have also checked with Monte Carlo test samples that the whole analysis chain is free of bias. Using the experimental values for the topological branching ratios deter-

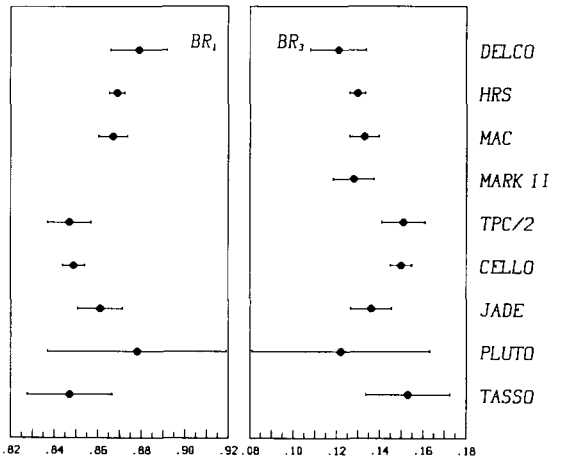

Fig. 1. Topological branching ratios BR_1 und BR_3 for the τ lepton from the various e^+e^--experiments (DELCO [17], HRS [15,16], MAC [14], TPC [11], MARK II [18], JADE [12], PLUTO [13], TASSO [10]).

mined above as input, the τ Monte Carlo simulation accurately describes the distribution of the events in the different charge topologies as shown in table 4. In order to estimate the systematic uncertainty of the efficiency matrix we studied various differential event distributions for data and Monte Carlo. From these comparisons and from the overall consistency between data and Monte Carlo (see table 4) we estimate the systematic error of the individual matrix elements to about 2%.

Table 4
Fractions of expected and observed events in the different topology classes for the 35 GeV data. For this consistency check the topological branching ratios used in the Monte Carlo simulation are taken from the data.

Topology	Monte Carlo [%]	Data [%]
1-1	64.38±0.48	64.51±1.42
1-2	11.56±0.21	11.10±0.60
1-3	19.93±0.27	20.00±0.83
1-4	0.89±0.06	1.01±0.26
1-5	0.18±0.03	0.18±0.08
2-3	1.42±0.01	1.69±0.25
3-3	1.23±0.01	1.40±0.20

To study the systematic uncertainties of the branching ratios due to our cuts we varied the selection criteria over a wide range. As an example, we have chosen four different sets of selection cuts and repeated the whole analysis procedure. We show in table 5 the observed topology distributions and resulting branching ratios after simultaneously tightening the cuts for the minimal acoplanarity angle α_{acop} from 0° and 2° and for the upper limit of the calorimeter energy from $0.75\sqrt{s}$ to $0.5\sqrt{s}$ in roughly equidistant steps. The results of this investigation show that the systematic bias due to our selection cuts is well below 0.2%. The systematic errors for the branching ratios are finally determined by varying all the efficiency matrix elements, including scanning and trigger inefficiencies, used in the likelihood fit (eq. (2)) within their combined statistical and systematic errors. This procedure yields a systematic error of 0.3% for the one-prong and three-prong branching ratios.

3.2. Cross sections and asymmetries

In the standard model [1], the lowest order differ-

Table 5
Observed events in the various charge topologies, and resulting branching ratios and total cross sections R_τ for four different sets of event selection cuts at $\sqrt{s}=35$ GeV (see text). Set 1 is the standard cut set.

Topology	Cut sets			
	1	2	3	4
1-1	1991±44.6	1711±41.4	1483±38.5	1318±36.3
1-2	319±17.9	288±17.0	242±15.6	212±14.6
1-3	590±24.3	524±22.9	453±21.3	403±20.1
1-4	30± 5.5	27± 5.2	24± 4.9	23± 4.8
1-5	6± 2.4	6± 2.4	6± 2.5	4± 2.0
2-3	53± 7.3	48± 6.9	37± 6.1	33± 5.7
3-3	43± 6.5	32± 5.6	27± 5.2	24± 5.0
sum	3032±55.1	2636±51.3	2272±47.7	2017±44.9
signal / background	13.1	21.7	25.3	31.3
R_τ	0.98±0.02±0.02	1.00±0.02±0.02	0.98±0.02±0.03	0.98±0.02±0.03
BR_1 [%]	85.0 ±0.5 ±0.3	84.9 ±0.5 ±0.4	84.9 ±0.6 ±0.4	84.9 ±0.6 ±0.5
BR_3 [%]	14.9 ±0.5 ±0.3	14.9 ±0.5 ±0.4	14.8 ±0.6 ±0.4	14.8 ±0.6 ±0.5
BR_5 [%]	0.16±0.13±0.04	0.20±0.14±0.07	0.26±0.15±0.08	0.25±0.15±0.08

ential cross section for τ pair production, as a function of the polar angle θ, is given by

$$\frac{\mathrm{d}\sigma}{\mathrm{d}\cos\theta}(\mathrm{e}^+\mathrm{e}^-\to\tau^+\tau^-) = \frac{\pi\alpha^2}{2s}[C_1(s)(1+\cos^2\theta)+C_2(s)\cos\theta], \quad (4)$$

with

$$C_1(s)=1+2v_e v_\tau \mathrm{Re}\,\chi(s) + (v_e^2+a_e^2)(v_\tau^2+\sigma_\tau^2)|\chi(s)|^2,$$
$$C_2(s)=4a_e a_\tau \mathrm{Re}\,\chi(s)+8v_e a_e v_\tau a_\tau|\chi(s)|^2,$$
$$v_e=v_\tau=-1+4\sin^2\theta_W,$$
$$a_e=a_\tau=-1, \quad (5)$$

and $\chi(s)$ given in the so-called "on-shell" renormalization scheme as

$$\chi(s)=\frac{1}{16\sin^2\theta_W\cos^2\theta_W}\frac{s}{s-M_Z^2+\mathrm{i}\Gamma_Z M_Z}, \quad (6)$$

where $\sqrt{s}$ is the centre of mass energy, M_Z and Γ_Z are the mass and width of the Z^0 intermediate vector boson and θ_W is the Weinberg angle. The terms proportional to $\mathrm{Re}\,\chi(s)$ arise from the interference between γ and Z^0 exchange and those proportional to $|\chi(s)|^2$, from the direct Z^0 exchange. The forward–backward asymmetry in the differential cross section is given as:

$$A_\tau=\frac{\int_0^1(\mathrm{d}\sigma/\mathrm{d}\cos\theta)\mathrm{d}\cos\theta-\int_{-1}^0(\mathrm{d}\sigma/\mathrm{d}\cos\theta)\mathrm{d}\cos\theta}{\int_{-1}^1(\mathrm{d}\sigma/\mathrm{d}\cos\theta)\mathrm{d}\cos\theta} = \tfrac{3}{8}C_2(s)/C_1(s). \quad (7)$$

At energies relevant for this experiment, A_τ can be approximated with an accuracy of better than 1% by

$$A_\tau=\tfrac{3}{2}a_e a_\tau \mathrm{Re}\,\chi(s). \quad (8)$$

With $\sin^2\theta_W=0.23$ and $M_Z=93$ GeV, the standard model predicts -8.8%, -11.5%, and -15.5% for the lepton charge asymmetry at the centre of mass energies 35.0, 38.1, and 43.8 GeV, respectively.

The total cross section σ_τ relative to the lowest order QED cross section $\sigma_0=4\pi\alpha^2/3s$ is given by

$$R_\tau=\sigma_\tau/\sigma_0=C_1(s), \quad (9)$$

where σ_τ is connected to N_{tot} (eq. (1)), which we obtain from our fit, and to the measured luminosity L, by

$$\sigma_\tau=N_{\mathrm{tot}}/(L\cdot r_{\mathrm{QED}}). \quad (10)$$

r_{QED} is the radiative correction factor, mainly due to initial state radiation. The factors r_{QED}, which increase with the CM energy, have been calculated by Monte Carlo methods.

As a result we obtain the cross sections σ_τ and the ratios R_τ shown in table 6 for the different energy regions. The systematic errors given in the table contain contributions from the luminosity determination (3%), the background subtraction (2%), the radiative correction (0.2%) and overall efficiency uncertainties (2%), as well as contributions due to the trigger, the selection criteria, the Monte Carlo simulation and scanning (in total 3%).

The measured values agree well with the standard model and the QED expectation (fig. 2). For $\sin^2\theta_W=0.23$ one expects an excess of 0.8% over σ_0 at energies $\sqrt{s}\cong 43$ GeV due to Z^0-exchange. The measurement errors of 3%, however, do not allow us to discriminate this additional contribution in the cross section from the pure QED cross section.

One can translate the measurement of R_τ into a limit for the charge radius of the τ. With the parametrization

$$\sigma_\tau=\sigma_0\left(1\mp\frac{s}{s-\Lambda_\mp^2}\right)^2 \quad (11)$$

we get $\Lambda_->231$ GeV and $\Lambda_+<318$ GeV at 95% CL. This corresponds to an upper limit of the τ charge radius of 2.1×10^{-3} fm.

To determine the charge asymmetry A_τ, we have used the event sphericity axis to estimate the τ scattering angle and have verified by Monte Carlo calculations that by this method, at our energies, the τ direction of flight is approximated to better than 1.9°.

In the on-shell renormalization scheme the charge asymmetry only has to be corrected for pure QED radiative effects at least within the accuracies of our experimental results, since the QED radiative corrections to the Z^0 exchange happen to cancel the one loop corrections to the Z^0 propagator at our energies [21].

The charge asymmetry has been determined in a likelihood fit where also the expected differential

Table 6
Cross sections for τ-pair production.

$\sqrt{s}$ [GeV]	L [pb^{-1}]	Events	r_{QED} [a]	σ_τ [pb]	R_τ
14.0	1.01±0.03	234	1.23	483 ±32 ±17	1.09±0.07±0.06
22.0	2.48±0.08	186	1.28	183 ±14 ± 6.9	1.02±0.08±0.04
34.2	11.30±0.34	434	1.33	76.7± 3.7± 5.1	1.03±0.05±0.07
35.0	87.00±1.74	3032	1.34	69.5± 1.3± 1.5	0.98±0.02±0.02
38.1	8.62±0.18	260	1.36	59.6± 3.9± 2.6	0.99±0.06±0.04
41.1	4.18±0.11	88	1.37	49.9± 5.5± 2.5	0.97±0.11±0.05
43.6	18.38±0.38	376	1.38	43.8± 2.3± 1.8	0.96±0.05±0.04
44.2	12.98±0.21	266	1.38	43.0± 2.8± 1.7	0.97±0.06±0.04
46.1	4.55±0.10	94	1.38	48.1± 5.2± 2.2	1.17±0.13±0.05

[a] r_{QED} = radiative correction from QED.

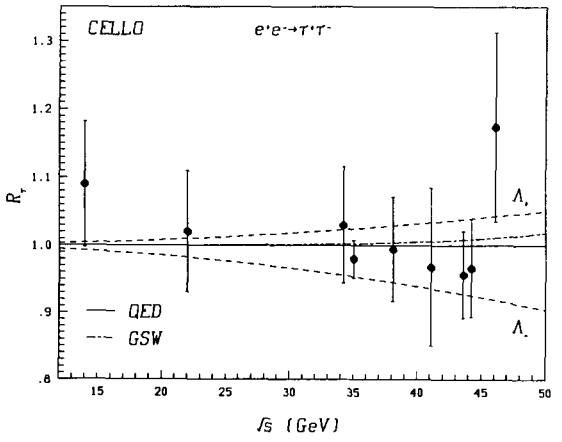

Fig. 2. Measurement of the total cross section R_τ with the CELLO detector. The dashed lines correspond to 95% CL lower limits on the parameters $\Lambda_\pm$ used to describe the τ charge radius.

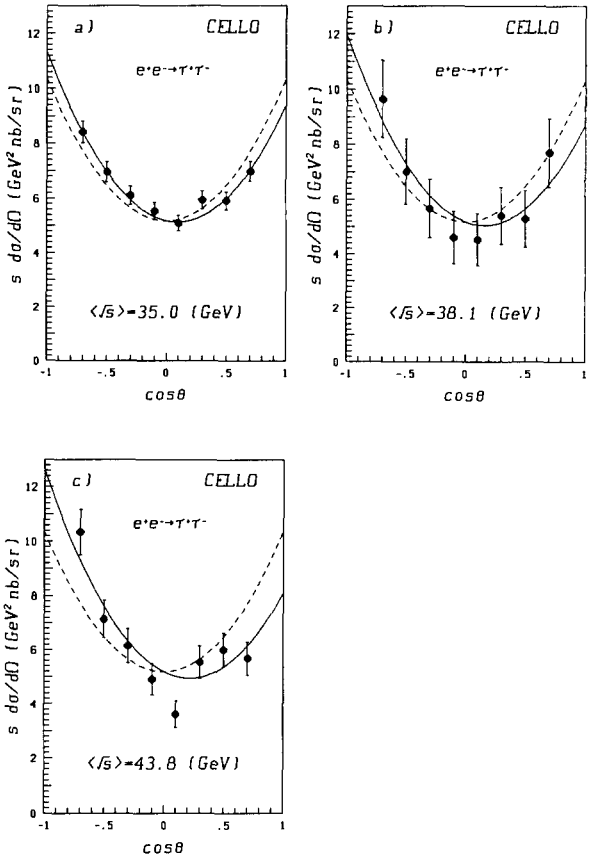

Fig. 3. Measurements of the differential cross section for τ pair production at $\sqrt{s}$=35.0 GeV (a), $\sqrt{s}$=38.1 GeV (b), and $\sqrt{s}$=43.8 GeV (c). The full lines show the results of fits allowing for an angular asymmetry and the dashed lines the symmetric QED expectation.

background contributions and the differential radiative correction factors have been taken into account. We have evaluated the residual background from the reactions $e^+e^-\to e^+e^-$ $(n\gamma)$, $n\geq 0$ which, due to their strong positive charge asymmetry, will bias the τ lepton asymmetry towards smaller absolute values. This background was estimated by subjecting Monte Carlo generated Bhabha events to a complete simulation of our analysis chain. The generator is based on a standard generator for $e^+e^-\to e^+e^-(\gamma)$ [22] using a further method proposed by Yennie, Frautschi and Suura [23] and Jadach [24] to add further radiative photons to the final state.

The angular distribution for τ pair production, corrected for radiative effects and background contributions, are shown in fig. 3 for $\sqrt{s}$=35.0, 38.1 and

43.8 GeV, respectively. The values of the charge asymmetry for the three energy bins and earlier CELLO measurements are shown in fig. 4 and listed in table 7. The measurements are all in good agreement with the expectations from the standard model. The systematic errors for the three new asymmetry measurements given in the table include the uncertainties from the radiative corrections (0.7%) and the background contributions (0.9%). The results from the likelihood fit have been cross-checked with various other methods such as fits to the binned angular distributions, counting events in forward and backward directions, and calculating weights. We obtain consistent results with all these methods [7].

Taking together all CELLO measurements of σ_τ and A_τ (tables 6, 7) and assuming the validity of the standard model, we performed a common fit to σ_τ and A_τ to determine the weak coupling constants v_τ and a_τ. Using $v_e = -0.088 \pm 0.072$ and $a_e = -0.996 \pm 0.054$ from neutrino electron scattering [25,26] we obtain (see e.g. refs. [7,27] for details of the fitting procedure)

$$v_\tau = -0.99 \pm 2.45\,,$$
$$a_\tau = -0.88 \pm 0.23\,, \qquad (12)$$

which is consistent with the expectation from the standard model of $a_\tau = -1$ and $v_\tau = -0.08$ ($\sin^2\theta_W = 0.23$). With the result for v_τ from the CELLO polarisation measurement [28], v_τ can be improved to $v_\tau = -0.6 \pm 1.8$, in agreement with a recent measurement by MAC [29]. If we assume universality, i.e. $v = v_e = v_\tau$, $a = a_e = a_\tau$ the result of the fit is

$$v^2 = 0.17 \pm 0.28\,,$$
$$a^2 = 0.88 \pm 0.23\,. \qquad (13)$$

These values are compatible with results from other experiments [12,30,16].

Alternatively, fixing a_e and a_τ to -1 as expected in the standard model, we have determined $\sin^2\theta_W$ from our data and obtain, in good agreement with other measurements (see e.g. refs. [26,31]), $\sin^2\theta_W = 0.25 \pm 0.05 \pm 0.01$, where the second error is due to the uncertainty in the Z^0 mass.

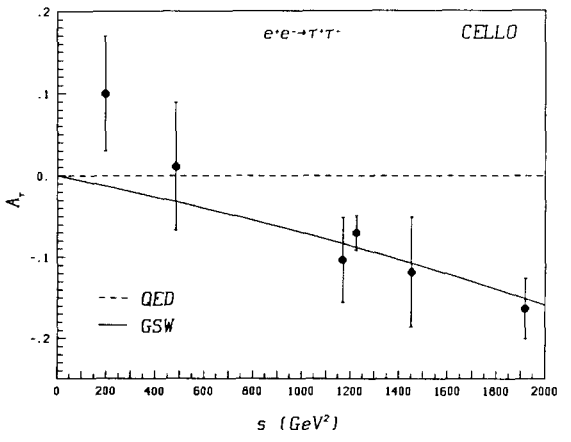

Fig. 4. Measurements of the charge asymmetry parameter A_τ with the CELLO detector.

Table 7
Charge asymmetries for τ pair production.

$\sqrt{s}$ [GeV]	Events	A_τ [%]	A_{GSW} [%]	Ref.
14.0	234	10.0 ± 7.0	-1.3	[5]
22.0	186	1.1 ± 7.8	-3.2	[5]
34.2	434	-10.3 ± 5.2	-8.5	[3]
35.0	3032	$-7.0 \pm 1.9 \pm 0.9$	-8.8	a)
38.1	263	$-11.8 \pm 6.2 \pm 2.7$	-11.5	a)
43.8	813	$-16.3 \pm 3.5 \pm 1.3$	-15.5	a)

a) This analysis.

4. Conclusion

Our results for the cross section and charge asymmetry in τ-pair production show good agreement with the expectations from the standard model. The measured values for the weak charges are consistent with the hypothesis of universal coupling of the weak neutral current to all sequential leptons.

We have improved and reconfirmed our previous measurements of the topological branching ratios. The precision of our new measurements is similar to that of the high statistics experiments at PEP [14–16]. Compared with these experiments, we observe a significantly smaller branching ratio for one-prongs and, correspondingly, a significantly larger branching ratio for three-prongs. The difference is 3.4 standard deviations in comparison with the previous world average. These results are interesting in con-

nection with the problem of the "missing" one prong decays, with arises when the sum of exclusive channels yielding a single charged particle are compared with the topological one-prong branching ratio [2]. Since in many experiments the exclusive decay channels have been normalised to the three-prong branching ratio due to the fact that τ pair candidates have been searched for only in events where a one-prong recoils against a three-prong, a too low value of the three-prong branching ratio may be partially responsible for the large fraction of "missing" exclusive one-prong decays [32]. Our measurements, indicating a larger three-prong branching ratio, may thus be viewed as a step towards a consistent interpretation of the τ decay pattern. We are further pursuing the question of missing exclusive decay channels by measuring the various decay modes, in particular those involving additional π^0's.

Acknowledgement

We gratefully acknowledge the outstanding efforts of the PETRA machine group which made possible these measurements. We are indebted to the DESY computer centre for their excellent support during the experiment. We acknowledge the invaluable effort of the many engineers and technicians from the collaborating institutions in the construction and maintenance of the apparatus. The visiting groups wish to thank the DESY Directorate for the support and kind hospitality extended to them.

This work was partially supported by the Bundesministerium für Forschung und Technologie (Germany), by the Commissariat à l'Energie Atomique and the Institut National de Physique Nucléaire et de Physique des Particules (France), by the Istituto Nazionale di Fisica Nucleare (Italy), by the Science and Engineering Research Council (UK), and by the Ministry of Science and Development (Israel).

References

[1] S.L. Glashow, Nucl. Phys. 22 (1961) 579; Rev. Mod. Phys. 52 (1980) 539;
A. Salam, Phys. Rev. 127 (1962) 1331; Rev. Mod. Phys. 52 (1980) 525;
S. Weinberg, Phys. Rev. Lett. 19 (1967) 1264; Rev. Mod. Phys. 52 (1980) 515.
[2] F.J. Gilman and S.H. Rhie, Phys. Rev. D 31 (1985) 1066; F.J. Gilman, SLAC report SLAC-PUB-4265 (1987).
[3] H.J. Behrend et al., Phys. Lett. B 114 (1982) 282.
[4] H.J. Behrend et al., Z. Phys. C 23 (1984) 103.
[5] V. Journé, Etude de la production et de la désintégration de paires $\tau^+\tau^-$ à PETRA, Thèse de Doctorat d'État, Université de Paris-Sud (1984), report LAL 84/20.
[6] CELLO Collab. H.J. Behrend at al., Phys. Scr. 23 (1981) 610.
[7] W. Wiedenmann, Messung elektroschwacher Effekte und topologischer Verzweigungsverhältnisse in der Reaktion $e^+e^-\to\tau^+\tau^-$ am Speicherring PETRA, report MPI-PAE/Exp. El. 195 (1988).
[8] S. Jadach, Acta Phys. Pol. B 16 (1985) 1007.
[9] B.C. Barish and R. Stroynowski, Phys. Rep. 157 (1988) 1.
[10] TASSO Collab. M. Althoff et al., Z. Phys. C 26 (1985) 521.
[11] TP Collab., A. Aihara et al., Phys. Rev. D 35 (1987) 1553.
[12] JADE Collab., W. Bartel et al., Phys. Lett. B 161 (1985) 188.
[13] PLUTO Collab., Ch. Berger et al., Z. Phys. C 28 (1985) 1.
[14] MAC Collab., E. Fernandez et al., Phys. Rev. Lett. 54 (1985) 1624.
[15] HRS Collab., C. Akerlof et al., Phys. Rev. Lett. 55 (1985) 570.
[16] HRS Collab., K.K. Gan et al., Phys. Lett. B 153 (1985) 116.
[17] DELCO Collab., W. Ruckstuhl et al., Phys. Rev. Lett. 56 (1986) 2132.
[18] MARK II Collab., M.E. Levi et al., Phys. Rev. Lett. 51 (1983) 1941.
[19] I. Beltrami et al., Phys. Rev. Lett. 54 (1985) 1775.
[20] B.G. Bylsma et al., Phys. Rev. D 35 (1987) 2269.
[21] M. Böhm and W. Hollik, Phys. Lett. B 139 (1984) 213.
[22] F.A. Berends and R. Kleiss, Nucl. Phys. B 228 (1983) 573.
[23] D.R. Yennie, S.C. Frautschi and H. Suura, Ann. Phys. (NY) 13 (1961) 379.
[24] S. Jadach, preprint MPI-PAE/PTh 6/87 (1987).
[25] W. Krenz, preprint PITHA 84/42 (March 1985).
[26] U. Amaldi et al., Phys. Rev. D 36 (1987) 1385.
[27] CELLO Collab., H.J. Behrend et al., Phys. Lett. B 191 (1987) 209.
[28] CELLO Collab., H.J. Behrend et al., Phys. Lett. B 127 (1983) 270.
[29] W.T. Ford et al., Phys. Rev. D 36 (1987) 1971.
[30] E. Fernandez et al., Phys. Rev. Lett. 54 (1985) 1620.
[31] C. Kiesling, Tests of the standard theory of electroweak interactions, Springer Tracts in modern Physics, Vol. 112 (Springer, Berlin, 1988).
[32] C. Kiesling, in: High energy electron–positron physics, eds. A. Ali and P. Söding (World Scientific, Singapore, 1988); K.K. Gan and M.L. Perl, Intern. J. Mod. Phys. A 3 (1988) 531;
K.G. Hayes and M.L. Perl, Phys. Rev. D 38 (1988) 3351.